

Effect of S adsorption on magnetic Co(0001) surface: a DFT study

S.H. Ma^{1,2}, X.T. Zu^{1,a}, Z.Y. Jiao², and H.Y. Xiao¹

¹ Department of Applied Physics, University of Electronic Science and Technology of China, Chengdu 610054, P.R. China

² College of Physics and information Engineering, Henan Normal University, Xinxiang, Henan 453007, P.R. China

Received 7 September 2007 / Received in final form 20 December 2007

Published online 29 February 2008 – © EDP Sciences, Società Italiana di Fisica, Springer-Verlag 2008

Abstract. Extended density functional theory calculations with the spin interpolation formula of Vosko, Wilk, and Nusair (VWN) are employed to study the effect of atomic S adsorption on Co(0001) surface. Besides the site preference for atom S in fcc-hollow site and adsorption geometry structures are in good agreement with experiments and previous calculations, some differences are also reported for the geometry of S in hcp-hollow site. Moreover, vibrational frequency, magnetic moments and electronic structure analysis are presented in more detail.

PACS. 68.43.Bc Ab initio calculations of adsorbate structure and reactions – 68.43.Fg Adsorbate structure

1 Introduction

As compared to theoretical studies of adsorption on paramagnetic transition-metal (TM) systems, recently various adsorbates on magnetic surfaces of iron and cobalt have received much attention [1–8] (and references therein). In particular, sulfur, as one of the most common poison elements in catalytic reactions, adsorption on Fe(100) and Fe(110) surfaces, has no significant effect on the surface magnetization based on density functional theory calculations [1,2]. On the other magnetic Co(0001) surface, Stépán et al. [5] have found that such adsorbates as atom H, C, and O not only prefer an antiferromagnetic (AF) coupling with the metallic Co substrate but also quench the magnetization at neighboring Co atoms differently through the tight-binding linear-muffin-tin-orbital (TB-LMTO) studies, e.g. atoms C and N reduce the magnetization of Co roughly twice, the effect of O is weaker. Besides that, it has been reported that molecule CH₃S with atom S directly bonding to Co(0001) surface, also does not quench the interface magnetism [7,8].

For atom S adsorption on Co(0001) surface, the most favored fcc-hollow site is observed by low energy electron diffraction (LEED) experiments and this has been confirmed by Lahtinen et al. [3] using the spin-polarized density functional theory (DFT) calculations. As a further study for S and CO co-adsorption on Co(0001) surface next, here we first study the interaction of S with Co(0001) substrate with a $p(2 \times 2)$ overlayer and have pre-

sented more details for geometry, vibrational frequency as well as the electronic structures. Differently, in this study we consider the spin interpolation formula of Vosko et al. (VWN) [9], which is well known to give reasonable results for the magnetic properties [10].

2 Computational method

All spin-polarized first-principles density functional theory (DFT) calculations with the spin interpolation formula of Vosko et al. (VWN) [9] were carried out using the projector augmented-wave (PAW) potentials [11,12] and the Perdew-Wang (PW91) generalized gradient approximations (GGA) functional [13] for electronic exchange-correlation interaction, as implemented in the Vienna *ab initio* simulation package (VASP) [14,15]. The energy cut-off was set at 335 eV for all calculations.

The ferromagnetic Co(0001) surface was simulated by a seven-layer slab separated by a vacuum thickness of 14 Å with sulfur adsorbed on one side of the slab. Only the bottom two layers of Co atoms were fixed at the bulk truncated positions, while other layers and adatom S were relaxed freely within the conjugate-gradient (CG) method until the convergence in electronic energy was 1.0×10^{-4} eV and the Hellmann-Feynman forces on the atoms were less than about 0.02 eV/Å. A Γ -centered Monkhorst-Pack grid of $8 \times 8 \times 1$ and a Methfessel-Paxton smearing with $\sigma = 0.2$ eV were adopted for the Brillouin zone integrations and all energies have been extrapolated to $T = 0$ K.

^a e-mail: xtzu@uestc.edu.cn

Table 1. The surface energy σ , interlayer relaxations Δd_{ij} (in percent) and layer projected magnetic moments $\mu(\mu_B)$ for clean Co(0001). Previous DFT results and experimental values are given for comparison.

	σ (J/m ²)	Δd_{12}	Δd_{23}	Δd_{34}	magnetic moments $\mu(\mu_B)$				
					S	S-1	S-2	S-3	bulk
This work	2.13	-3.0	+1.1	-0.2	1.73	1.65	1.61	1.62	1.59
[7,8]	2.1	-3.0	+0.6	-0.1	1.76	1.70	1.66		1.61
[3]	2.16	-3.0	+0.8		1.70				1.66
[5]					1.70	1.62	1.62	1.63	1.60
Exp.	1.88 ^a	-2.1 ^b	+1.3 ^b	-0.2 ^b					1.58 ^a

The subscripts indicate the layers, 1 being the topmost one, etc. S: surface, layer; S-1: subsurface; S-2: the third S-3: the central layer.

^{a,b} Experimental values taken from Reference [8] and [17], respectively.

Reference [3]: PAW-PW91 calculations without the VWN formalism.

Reference [5]: TB-LMTO calculations.

Reference [7,8]: US-PP calculations.

Based on the optimized structures, vibrational frequencies for S are determined by diagonalizing Hessian matrix with displacements of 0.02 Å using finite differences keeping the substrate fixed (allowing only the S atom to move). We have applied the calculated equilibrium bulk lattice values $a = 2.488$ Å and $c/a = 1.623$, which fit well with the experimental values $a = 2.507$ and $c = 4.070$ Å [16], giving $c/a = 1.62$. Convergence of calculations (energy cutoff, k -point tests etc.) has been carefully tested to provide a good compromise between accuracy and computational efficiency.

3 Results and discussion

3.1 The clean Co (0001) surface

As a further check on the accuracy, we first calculate the surface relaxation, surface energy and magnetic properties for clean Co(0001) surface and the results are summarized in Table 1, which agree well with the previous calculations [3,5,7,8] and experimental values [17]. In the surface (S) layer, the magnetic moment for Co atoms is enhanced to $1.69\mu_B$ with respect to the bulk value of $1.59\mu_B$ as a consequence of coordination reduction from a 3D to a 2D system and the narrowing of $3d$ -orbital of Co atoms on clean surface (see Fig 1a). From the subsurface (S-1) to the central (S-3) layer, the magnetic moments are of 1.62 and $1.59\mu_B$, respectively, in agreement with previous studies [5,7,8]. The present magnetic moments are generally less than those obtained from the ultrasoft pseudopotential (US-PP) calculations [7,8], maybe due to the difference for the ion-electron interaction between PAW and US-PP.

The density of states (DOS) for clean Co(0001) surface are also shown in Figure 1, along with that of bulk Co for comparison. Only the DOS of surface layer is different from that of bulk between energies of -1.0 to -3.0 eV for the majority spin and near -1.0 eV for the

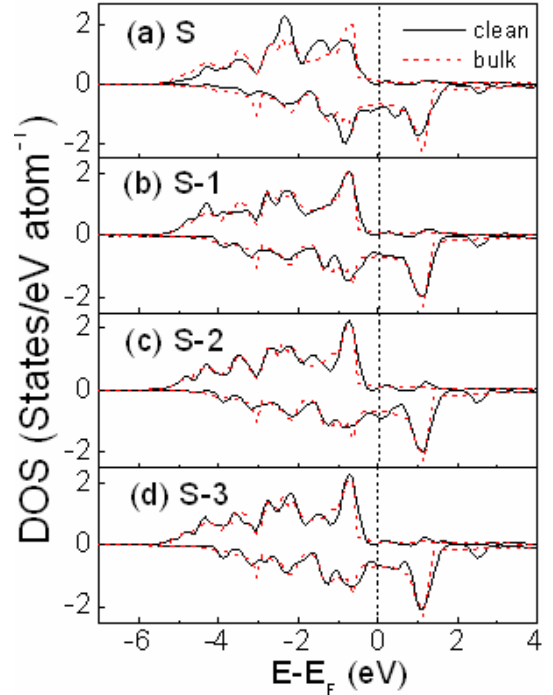


Fig. 1. Layer projected density of states (LDOS) for clean Co(0001) slab (solid lines) compared with that of bulk Co atom (dashed lines); positive (negative) values indicate spin-up (spin-down). Fermi levels are shifted to zero for all cases. (Only $3d$ -orbital of cobalt are shown here and below since the s , p -orbital contribution are negligible in considered energy region.)

minority spin. The DOS for the minority-spin near E_F is larger than that for the majority-spin, therefore inducing a positive spin asymmetry according to the definition of reference [5]. Other layers show a bulklike DOS from Figure 1b, 1c and 1d.

Table 2. The results for S /Co(0001) system with a p (2 × 2) overlayer for S adsorption in different sites.

	Fcc	Reference [3]		Hcp	Reference [3]		Bridge	Reference [3]		Atop	Reference [3]	
E_{ads} (eV)	5.29	5.35		5.26	5.33		5.09	5.15		4.033	4.12	
d_{12}	1.986	1.98	2.05^{Exp}	1.993	1.96		1.982	1.98		2.007	1.97	
d_{23}	2.046	2.01	2.03^{Exp}	2.042	2.02		1.995	2.02		2.043	2.02	
d_{34}	2.016			2.016			2.020			2.017		
$h_{S-Co(I)}$	1.62	1.61	1.59 ± 0.06^{Exp}	1.60	1.57		1.67	1.66		2.02	2.02	
$h_{S-Co(II)}$	1.65	1.64		1.64	1.60		1.56	1.57		1.86	1.87	
h_{S-Co}	2.14			2.13			2.07			2.02		
z_1	0.03	0.03		0.03			0.09			0.09		
z_2	0.06						0.06			0.01		
v_z	345			332			346			381		
v_x	199			203			242			110*		
v_y	197			189			85*			125*		

The adsorption energy E_{ads} is calculated according to: $E_{ads} = (E_{Co(0001)} + E_S) - E_{S/Co(0001)}$; d_{ij} : the interlayer spacing; d_{S-Co} : the nearest S-Co bond distance; $h_{S-Co(I)}$ and $h_{S-Co(II)}$ are the vertical distances between S and the nearest neighbor Co(I), next nearest Co(II) atoms on the surface layer; z_1 , z_2 are the buckling in the surface and subsurface layer; The translational v_x , v_y and stretching v_z vibrational frequencies are in unit of cm^{-1} . * indicates an imaginary frequency. All structure parameters are in Å.

3.2 S adsorption on Co(0001) surface

3.2.1 Adsorption energy, geometry and vibrational frequency analysis

Table 2 presents the calculated values for high symmetry adsorption sites along with the previous results. It can be seen that quantitative agreement with reference [3] is achieved. Our predicted binding energies are generally lower than the results without VWN formula [3]. The most favorable site is fcc-hollow with a binding energy of 5.29 eV, leading the hcp-hollow site by 30 meV, followed by the bridge and atop sites. Upon S adsorption, complex relaxations of the substrate occur, including the lateral and vertical relaxations (the buckling of the substrate layers). In fcc-hollow site, the three nearest-neighbor Co(I) atoms laterally moved by 0.033 Å away from S atom, in confirmation of the experimental and the theoretical values of 0.05 ± 0.09 Å and 0.03 Å, respectively [3]. However, we do note one deviation from reference [3], in hcp-hollow site our calculations also show a larger lateral displacements of 0.055 Å for nearest Co atoms away from S. On-atop site the movements of nearest Co atoms are negligible and on bridge site the most from the data in Figure 2. All these small displacements serve to allow S to get closer to the surface and to form stronger bonds, therefore result in the nearest S-Co bond distance d_{S-Co} being of 2.14, 2.07 and 2.02 Å for hollow, bridge and atop sites, respectively. These are related to the coordination number: the shortest for atop site directly bonding to only one atom, but longer for bridge and longest for hollow sites where the bonding is distributed over more atoms. Similarly, the vertical distances $h_{S-Co(I)}$ and $h_{S-Co(II)}$ between S and the neighbor Co(I), Co(II) atoms on the topmost layer, increase on

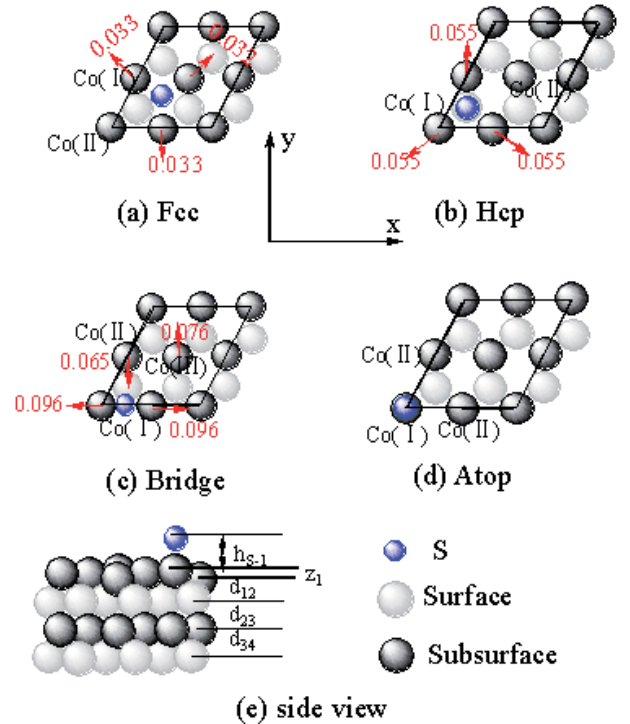


Fig. 2. Geometry for the S/Co(0001) system with atom S adsorbed in the high symmetry sites. The solid line is for p(2 × 2)-S unit mesh. The bottom (e) is for side view and the others for top views. The values for the displacements are in units of Å.

going from the three-fold hollow to the bridge and one-fold atop sites. As for the buckling in the first layer z_1 , the bridge and atop sites are the most with a buckling of 0.09 Å in comparison to that of 0.03 Å for both fcc- and

Table 3. Calculated magnetic moments (μ_B) for the topmost four layer Co atoms as well as atom S in different adsorption sites.

Site	Layer magnetic moment (μ_B)						
	S	(Reference [3])	S-1	S-2	S-3	Atoms S	
Fcc	Co(I)	1.47	(1.46)	1.57 ~ 1.68	1.60	1.58	0.056
	Co(II)	1.85	(1.84)		1.58	1.60	
Hcp	Co(I)	1.39	(1.37)	1.56 ~ 1.68	1.59	1.59	0.052
	Co(II)	1.81	(1.78)		1.57		
Bridge	Co(II)	1.35	(1.38)	1.57 ~ 1.64	1.57	1.58	0.066
		1.77	(1.76)				
Atop	Co(I)	1.31	(1.23)	1.56 ~ 1.65	1.59	1.59	0.17
	Co(II)	1.79	(1.78)				
Clean		1.73		1.65	1.61	1.62	1.59 ^{bulk}

The values in parenthesis are taken from reference [3]. For surface layer (S), the upper (lower) row shows magnetic moments at nearest Co(I) (next nearest Co(II)) atoms. For comparison, results for clean surface and bulk Co are displayed at the bottom of the table.

hcp-hollow sites. The subsurface layer is also buckled by 0.06 Å for S in fcc-hollow site, contrast to the negligible one in hcp-hollow site.

Vibrational frequency analysis for the adsorbate atoms on the surface can indicate the nature of the stationary points on the potential energy surface. As shown by the vibrational frequencies in Table 2, both the fcc- and hcp-hollow sites are the minimum with no imaginary frequencies. S in the bridge site is classified as a transition state, for which the imaginary frequency indicates that a symmetric movement in the y -direction will lead to the most energetically stable hollow site. Atop site is a second order saddle point with two imaginary frequencies and movement in the x - or y -directions along the surface will result in a transition state and then further to a more stable site. The magnitude of the stretching frequency ν_z is found to increase from the hollow site to the bridge and then the atop sites, in line with the calculated height of S above the surface $h_{S-Co(I)}$, and is also related to the S-Co coordination, being smaller for higher coordination sites. This trend is similar to S on magnetic Fe surfaces [1].

3.2.2 Magnetic moments

Table 3 lists the magnetic moments for different layers after S adsorption. For all adsorption sites, in surface layer nearest Co(I) atoms show a reduction in magnetic moment compared to that of the clean surface, whereas that for the next nearest Co(II) atoms increases to $\sim 1.80\mu_B$. These are also in agreement with those of reference [3]. Subsurface layer Co atoms have different magnetic moments and the differences from those in same layer of clean slab, indicate that the interaction of atom S extends as far as the second layer, while the magnetic moments for the third (S-2) and the central (S-3) layers compare well to the obtained bulk value of $\sim 1.60\mu_B$. These properties indicate S interacts

primarily with the surface and slightly with the subsurface layers.

At the other bulk-terminated layer, the magnetic moments are of $\sim 1.70\mu_B$, very close to the clean bulk-terminated value of $1.73\mu_B$. The induced magnetic moments on S are about 0.05, 0.07 and $0.17\mu_B$ for hollow, bridge and atop sites, respectively, indicating S ferromagnetically (parallel) coupling with substrate.

3.2.3 Density of states (DOS) and charge density difference

Firstly, the layer projected density of states (DOS) before and after S adsorption in fcc- and hcp-hollow sites are given in Figure 3. It can be seen that the DOS for the surface layer after S adsorption differ significantly from that of the clean surface and for the subsurface layer little change has happened. For the third and the subsequent layers, there is no discrepancy between the clean and S adsorbed surfaces. These are consistent with the effect of S on the magnetization upon S adsorption.

Furthermore, for inspection of the main interaction between S and the surface layer, we examined $3d$ -orbital DOS for the nearest neighbor Co(I) and the next nearest neighbor Co(II) atoms as well as $3p$ -orbital of S in Figure 4. For all adsorption sites below -3 eV with respect to the Fermi level, the bonding interaction between Co $3d$ -orbital and S $3p$ -orbital is quite strong. Near the Fermi level, the anti-bonding states between Co and S atoms are shown by a significant increase in the DOS of S atom. For the hollow sites adsorption, the S-induced changes in DOS for nearest atoms Co(I) (see (a) and (b) in Fig. 4) are slightly larger than that for Co(II) in energies from -3 eV to E_F , in line with the changes in magnetic properties of the two atoms.

Additionally, the differences of total DOS between S-covered and clean Co(0001) slabs in Figures 5a and 5b for

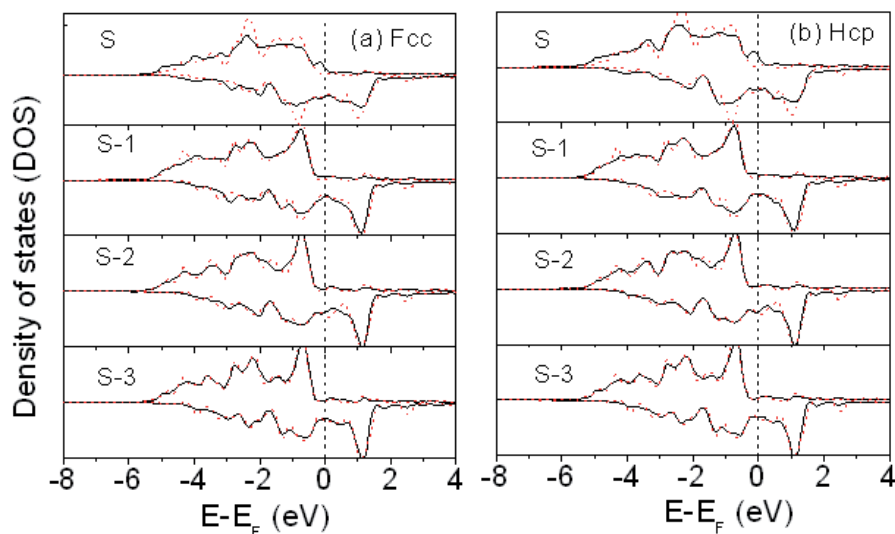


Fig. 3. Layer projected density of states (DOS) (in arbitrary unit) for S after (solid) and before (dot) adsorption in (a) fcc- and (b) hcp-hollow sites. S, S-1, S-2, S-3 are same as in Table 1

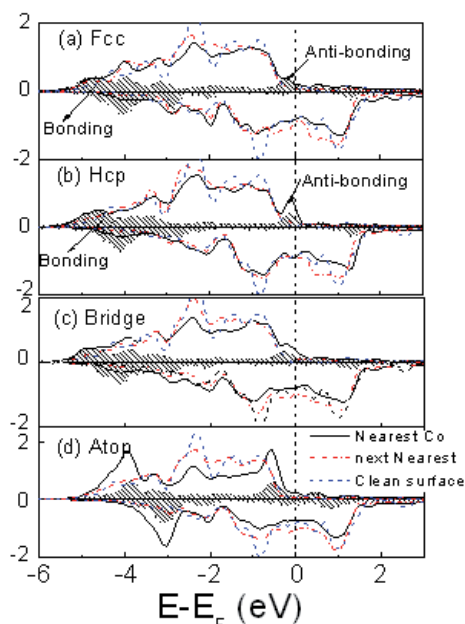


Fig. 4. Local 3d-orbital density of states (DOS) for nearest (solid line), next nearest (dash-dotted line) Co atoms in the surface layer compared to that in the clean surface (dashed line). The dashed area are for atom S .

fcc- and hcp-hollow sites, reflect that the bonding between atom S and its neighbor Co atoms is practically identical for both sites. And the bonding states for fcc-hollow site lies slightly at lower energy than that for hcp-hollow site, shown by the DOS difference between fcc- and hcp-hollow sites in Figure 5c. Moreover, S 3s orbital for the fcc-hollow site is located at -13.29 eV with respect to the Fermi level, somewhat deeper than for the hcp-hollow site where it is at -13.20 eV. These all contribute to S preference to the fcc-hollow site.

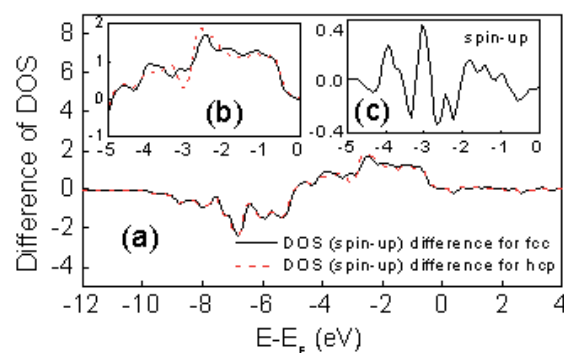


Fig. 5. The total DOS differences between the S-covered and clean Co(0001) is shown in (a). Inset (b) shows that from the Fermi level to -5 eV for clear inspection. Inset (c) shows DOS difference between fcc- and hcp-hollow sites (DOS of fcc minus that of hcp).

Lastly, charge density difference plots are shown in Figure 6 for S adsorbed in hollow sites. Some accumulation of charge is presented in the region between atom S and surface layer, and the charge is concentrated around atom S, indicating that S behaves as an electronegative species causing a transfer of charge from the surface to S. Moreover, some depletion of charge can also be seen around the second layer Co atoms although smaller, indicating that S does interact with the second layer.

4 Conclusion

The spin-polarized density functional theory calculations with spin interpolation formula of Vosko, Wilk, and Nusair (VWN) have been performed to study the effect of S adsorption on the magnetic Co(0001) surface. The fcc-hollow site is identified as the most favored site, in agreement

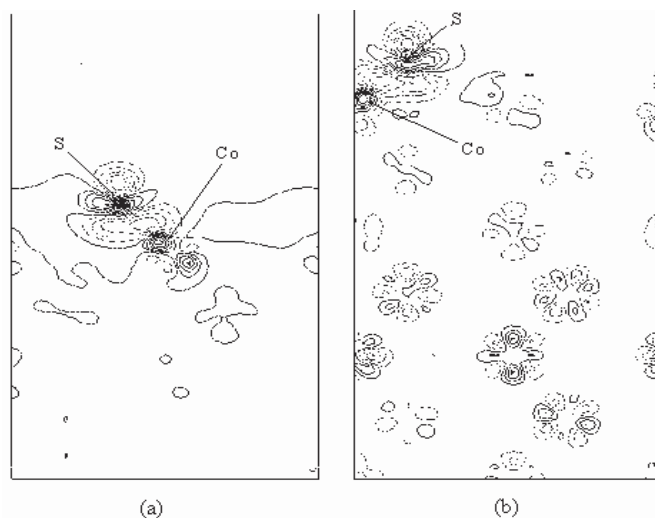


Fig. 6. Charge density differences for S adsorption in (a) fcc- and (b) hcp-hollow sites. The plots are in slices perpendicular to the surface normal (z) through the nearest and the next nearest Co atoms on the surface. The charge density difference is defined as: $\Delta\rho = \rho(S/Co(0001)) - \rho(Co(0001)) - \rho(S)$.

with the previous studies, however, two deviations are found for the adsorption geometry of S in hcp-hollow site: one is the lateral displacements of nearest Co atoms and the other is the buckling in surface layer. Vibrational frequency analysis show that the fcc- and hcp-hollow sites are the minimum, the bridge site is a transition state and atop site is a second order saddle point. The analysis for magnetic moments, density of states (DOS) and charge density difference indicate that S interacts strongly with the surface, somewhat with the subsurface. In different adsorption sites, the S-Co stretching frequency and the magnetic moments for Co and S atoms are related to the geometry and coordination number. The higher the coordination number, the less the magnetization for the nearest Co atoms gets quenched and the less the S moment is. Additionally, the induced magnetic moment on S atom although small shows the ferromagnetical coupling with Co(0001) surface. These trends are in accordance with those of atom O on the same surface with p (2×2) over-layer [5].

This work is supported financially by the Program for New Century Excellent Talents in University (NCET-04-0899) and by the Ph.D. Founding Support Program of Education Ministry of China (20050614013) and by Program for Innovative Research Team in UESTC.

References

1. N. Todorova, M.J.S. Spencer, I. Yarovsky, *Surf. Sci.* **601**, 665 (2007); S.G. Nelson, M.J.S. Spencer, I.K. Snook, I. Yarovsky, *Surf. Sci.* **590**, 63 (2005) (and references therein)
2. D.E. Jiang, E.A. Carter, *Surf. Sci.* **570**, 167 (2004)
3. J. Lahtinen, P. Kantola, S. Jaatinen, K. Habermehl-Čwirzeň, P. Salo, J. Vuorinen, M. Lindroos, K. Pussi, A.P. Seitsonen, *Surf. Sci.* **599**, 113 (2005)
4. K. Habermehl-Čwirzeň, J. Lahtinen, *Surf. Sci.* **573**, 183 (2004)
5. Š. Pick, H. Dreysse, *Surf. Si.* **540**, 389 (2003); *Surf. Si.* **474**, 64-70 (2001); *Surf. Sc.* **460**, 153 (2000)
6. J. Lahtinen, J. Vaari, K. Kauraala, E.A. Soares, M.A. Van Hove, *Surf. Sci.* **448**, 269 (2000)
7. L.G. Wang, E.Y. Tsymbal, S.S. Jaswal, *J. Magn. Magn. Mat.* **286**, 119 (2005)
8. L.G. Wang, E.Y. Tsymbal, S.S. Jaswal, *Phys. Rev. B* **70**, 075410 (2004)
9. S.H. Vosko, L. Wilk, M. Nusair, *Can. J. Phys.* **58**, 1200 (1980)
10. S. Denmler, J. Hafner, *Phys. Rev. B* **72**, 214413 (2005)
11. P. Blöchl, *Phys. Rev. B* **50**, 17953 (1994)
12. G. Kresse, D. Joubert, *Phys. Rev. B* **59**, 1758 (1999)
13. J.P. Perdew, J.A. Chevary, S.H. Vosko, K.A. Jackson, M.R. Pederson, D.J. Singh, C. Fiolhais, *Phys. Rev. B* **46**, 6671 (1992)
14. G. Kresse, J. Hafner, *Phys. Rev. B* **47**, R558 (1993); G. Kresse, J. Hafner, *Phys. Rev. B* **48**, 13115 (1993)
15. G. Kresse, J. Furthmuller, *Comput. Mater. Sci.* **6**, 15 (1996); G. Kresse, J. Furthmuller, *Phys. Rev. B* **54**, 11169 (1996)
16. Web Elements, the periodic table on the WWW, URL: www.webelements.com
17. J. Lahtinen, J. Vaari, T. Vaara, K. Kauraala, P. Kaukasoina, M. Lindroos, *Surf. Sci.* **425**, 90 (1999)
18. M.J.S. Spencer, I.K. Snook, I. Yarovsky, *J. Phys. Chem. B* **110**, 956 (2006); *J. Phys. Chem. B* **109**, 9604 (2005)